

Supplementary data of : Debris-flow surges of a very active alpine torrent : a field database

Suzanne Lapillonne^a, Firmin Fontaine^a, Frédéric Liebault^a, Vincent Richefeu^b, and Guillaume Piton^a

^aUniv. Grenoble Alpes, INRAE, CNRS, IRD, Grenoble INP, IGE, Grenoble, France

^bUniv. Grenoble Alpes, 3SR, Gières, France

Correspondence: Lapillonne Suzanne, (suzanne.lapillonne@inrae.fr)

1 Velocity determination

1.1 Cross-correlation method

Cross-correlations of two signals measures the displacement between those two signals that allows the maximal similarity between them. When using temporal signals of the same surge at two different position, this displacement is in fact a lag
5 between the two sensors (Fig. S1). This lag is a relevant indicator of the surge travel time from one sensor to the other. The cross-correlation is done on the signals normalized by their maximum value in order to be free from the choice of the pair of sensors, and their placement. Each event analysis is cross controlled visually. The indicator of similarity outputted by cross-correlation is used to validate the measurement. If the cross-correlation outputs an indicator of similarity that is too small, the alternative manual method defined below is used.

10 1.2 Manual method

Faulty sensors, very noisy signals or use of different sensor types may lead to the cross-correlation not being validated by the user. Alternatively, the lag is determined manually, thus relying more on user interpretation.

The method consists in the user determining the time stamps of any characteristic features of the time series for both signals, typically sharp fronts or maximum peak. It proved easier and more reliable to determine intervals in which the features are
15 contained than to locate a precise single instant. The mean lag is then computed based on these upper and lower bounds (Fig. S2). The uncertainty is determined by the bounds given by the user, and an added uncertainty given by the reading precision. On Figure S2, an example using the sharp front as a characteristic is shown.

2 Note on velocity calculation

The above mentioned method for calculating the velocity heavily relies on the assumption that the flow front is not decon-
20 structed between the two sensors. In the set up of the Réal torrent, the geophones inter-distances are relatively small considering

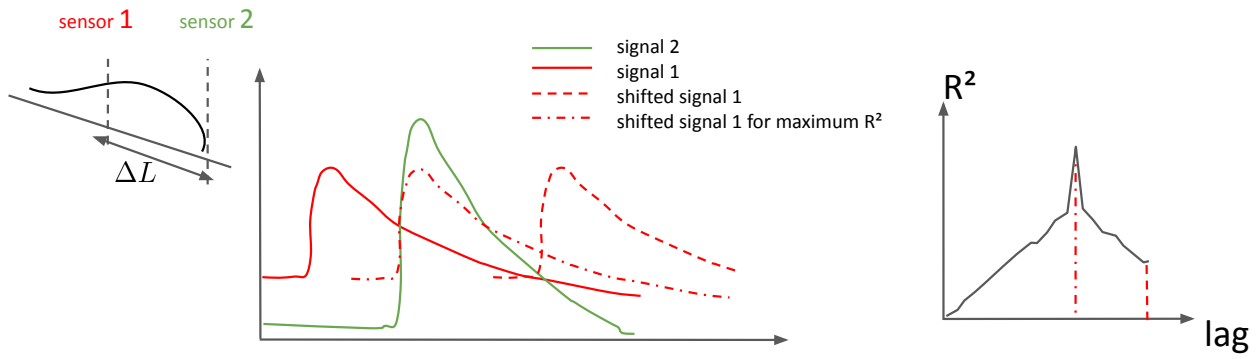


Figure S1. Velocity determination with the cross-correlation method

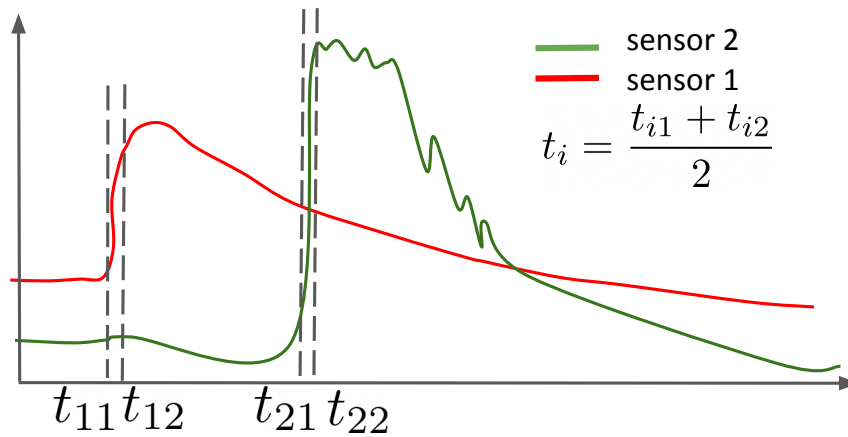


Figure S2. Velocity determination with the visual method

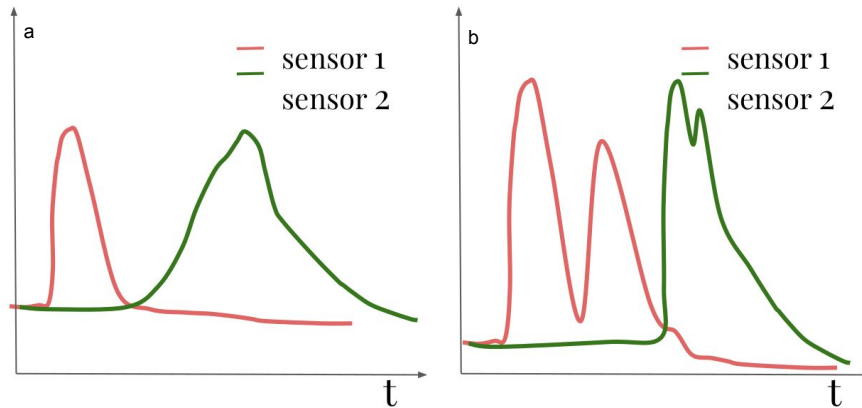


Figure S3. Special cases for the determination of the velocity : a) Change in the shape of the signal, b) Agglomeration of different surges

the average travel distance of a debris flow. However, it can occur that the debris-flow surge changes between the two sensors. Two cases will be discussed here :

- Changes in the shape of the surge,
- Successive surges agglomeration.

25 In the first case on Fig. S3a, a change in the shape of the geophone signal between the upstream and downstream geophones can be observed.

If this change is systematic through all the events, the difference is attributed to the difference in geological make ups around the geophones propagating differently the surge energy, and the velocity is computed by correlation. If the change is not systematic, the flow might have been deconstructed (especially if the geophones are placed around a check dam) and the
 30 velocity might be underestimated by the method described above. This case remains an outlier, and must be ruled out.

In the event of successive surges agglomerating as in Fig. S3b the surges are ignored in the current version of the protocol.

3 Uncertainty analysis

Uncertainties on each computed hydraulic parameters have been thoroughly propagated using the quadratic method and have been recorded in the database. The propagation of the error of the geophones on the lag was investigated and was determined
 35 to be negligible using the cross correlation method.

Uncertainties are not displayed on figures of this paper in order to avoid overloaded graphs. However, note that the error due to the hypothesis on the cross-section is the prevalent source of error on the volumes and Froude numbers, which is why the values for each hypothesis are saved into the database (see Table S1).

The cross section assumed to be of constant shape is an inherently flawed assumption, but the main interest of this process is to determine order of magnitudes of the volume, in which case this approximation should not influence in a significant way.

4 Dataset

Table S1. Dataset for each surges

Date	Station	Surge	Froude number [-]	Front Velocity [m/s]	Volume [m ³]	Volume (max hyp.) [m ³]	Volume (min hyp.) [m ³]	Maximal flow level [m]	Peak discharge [m ³ /s]	Peak discharge (max hyp.) [m ³ /s]	Peak discharge (min hyp.) [m ³ /s]	Rain intensity [mm/h]	Rain accumulati on [mm]
2011-06-29	S3	1	0,8	2,9	3718	5063	2373	1,349	39	43	35	19,7	3,3
2011-06-29	S2	1	0,8	3,4	1982	1987	1976	1,686	34	34	34	56,0	15,2
2011-06-29	S1	1	1,0	4,1	3040	3133	2947	1,729	41	42	40	79,6	26,1
2011-09-17	S2	1	0,5	1,7	1464	1557	1370	1,166	12	12	12	70,6	19,7
2011-09-17	S1	1	1,0	3,3	3348	3479	3216	1,062	19	19	18	60,3	21,7
2012-04-30	S2	1	0,8	2,7	3913	4459	1512	1,167	19	20	15	36,5	35,9
2012-04-30	S1	1	0,6	1,9	632	657	606	1,056	11	11	10	31,4	35,8
2012-04-30	S1	2	0,8	2,7	529	549	510	1,211	18	19	18	31,4	35,8
2012-04-30	S1	3	1,0	3,0	364	379	349	0,938	15	15	14	31,4	35,8
2012-04-30	S1	4	0,7	2,1	291	303	280	1,018	11	12	11	31,4	35,8
2012-05-27	S1	1	0,5	1,7	596	619	574	1,340	12	13	12	21,7	16,7
2013-03-30	S2	1	0,3	1,1	536	597	476	1,243	8	8	8	4,9	16,4
2013-03-30	S2	1											
2013-03-30	S1	1	0,3	1,0	305	316	293	1,146	6	6	6	4,8	17,5
2013-05-18	S1	1	0,4	1,2	405	420	391	1,111	7	8	7	9,6	57,1
2013-05-18	S1	2	0,5	1,9	559	577	542	1,635	18	19	18	9,6	57,1
2013-05-18	S1	3	0,5	1,9	663	683	643	1,536	16	17	16	9,6	57,1
2013-07-22	S1	1	0,6	2,4	1454	1502	1407	1,718	24	24	23	57,9	31,4
2014-01-04	S1	1	0,5	2,1	1241	1277	1205	2,174	28	28	28	7,2	5,8
2014-06-10	S3	2	1,6	6,3	3826	4116	2996	1,470	92	95	88	60,3	21,7
2014-06-10	S1	1	0,8	3,1	1295	1344	1247	1,595	28	28	27	72,4	28,9
2014-09-20	S2	1											
2014-09-20	S1	1	1,0	4,3	4475	4657	4293	1,790	45	46	44	74,8	15,9
2018-10-29	S3	1											
2018-10-29	S1	1	0,9	2,9	639	665	613	1,107	17	18	17	26,5	18,9
2019-12-01	S1	1	1,0	2,8	563	587	538	0,888	13	14	13	7,2	39,6
2019-12-01	S1	2	0,2	0,9	368	383	354	1,395	7	7	7	7,2	39,6
2019-12-19	S1	1	0,4	1,5	387	400	374	1,367	11	12	11	7,2	42,0
2019-12-19	S1	2	0,7	2,6	849	874	824	1,401	20	21	20	7,2	42,0
2019-12-19	S1	3	0,6	1,9	225	234	217	1,063	11	11	10	7,2	42,0
2019-12-19	S1	4	1,2	4,8	1106	1141	1072	1,682	46	47	45	7,2	42,0
2019-12-20	S1	1	0,5	1,8	381	396	365	1,104	10	11	10	7,2	15,1
2019-12-21	S1	1	1,2	4,9	1697	1756	1637	1,606	45	46	44	7,2	11,3
2020-06-07	S1	1	0,5	1,5	203	210	195	0,893	7	8	7	33,8	9,4
2020-06-13	S1	1	1,0	3,4	726	753	699	1,173	22	22	21	53,1	28,5